TECHNICAL REPORT ARBRL-TR-02579

RAMAN AND FLUORESCENCE SPECTROSCOPY IN A METHANE-NITROUS OXIDE LAMINAR FLAME

John A. Vanderhoff
William R. Anderson
Anthony J. Kotlar
Richard A. Beyer

August 1984

US ARMY ARMAMENT RESEARCH AND DEVELOPMENT CENTER
BALLISTIC RESEARCH LABORATORY
ABERDEEN PROVING GROUND, MARYLAND

Destroy this report when it is no longer needed.
Do not return it to the originator.

Additional copies of this report may be obtained from the National Technical Information Service, U. S. Department of Commerce, Springfield, Virginia 22161.

The findings in this report are not to be construed as an official Department of the Army position, unless so designated by other authorized documents.

The use of trade names or manufacturers' names in this report does not constitute indorsement of any commercial product.

UNCLASSIFIED

SECURITY CLASSIFICATION OF THIS PAGE *(When Data Entered)*

REPORT DOCUMENTATION PAGE		READ INSTRUCTIONS BEFORE COMPLETING FORM
1. REPORT NUMBER TECHNICAL REPORT ARBRL-TR-02579	2. GOVT ACCESSION NO.	3. RECIPIENT'S CATALOG NUMBER
4. TITLE *(and Subtitle)* Raman and Fluorescence Spectroscopy in a Methane-Nitrous Oxide Laminar Flame		5. TYPE OF REPORT & PERIOD COVERED Final 6. PERFORMING ORG. REPORT NUMBER
7. AUTHOR*(s)* John A. Vanderhoff, William R. Anderson, Anthony J. Kotlar and Richard A. Beyer		8. CONTRACT OR GRANT NUMBER*(s)*
9. PERFORMING ORGANIZATION NAME AND ADDRESS US Army Ballistic Research Laboratory ATTN: DRXBR-IBD Aberdeen Proving Ground, MD 21005-5066		10. PROGRAM ELEMENT, PROJECT, TASK AREA & WORK UNIT NUMBERS
11. CONTROLLING OFFICE NAME AND ADDRESS US Army Ballistic Research Laboratory ATTN: DRXBR-OD-ST Aberdeen Proving Ground, MD 21005-5066		12. REPORT DATE August 1984 13. NUMBER OF PAGES 41
14. MONITORING AGENCY NAME & ADDRESS*(If different from Controlling Office)*		15. SECURITY CLASS. *(of this report)* Unclassified 15a. DECLASSIFICATION/DOWNGRADING SCHEDULE

16. DISTRIBUTION STATEMENT *(of this Report)*

Approved for public release; distribution unlimited.

17. DISTRIBUTION STATEMENT *(of the abstract entered in Block 20, if different from Report)*

18. SUPPLEMENTARY NOTES

19. KEY WORDS *(Continue on reverse side if necessary and identify by block number)*

Flame Spectroscopy
Methane-Nitrous Oxide Flame
Raman
Fluorescence
Concentration Profile
Temperature Profile

20. ABSTRACT *(Continue on reverse side if necessary and identify by block number)* shg

Using the prism selected lines of argon and krypton lasers temperature and concentration profiles through the reaction zone of a premixed laminar methane-nitrous oxide flame have been obtained from the Raman signals for N_2, H_2O and CH_4. Fluorescence signals from NH, OH, CN and NCO have also been observed. These signals have been assigned to specific pumping transitions where possible and also converted to relative concentration profiles. Estimates of the absolute concentrations are also determined. Loss rates for

DD FORM 1 JAN 73 1473 EDITION OF 1 NOV 65 IS OBSOLETE

Unclassified

SECURITY CLASSIFICATION OF THIS PAGE *(When Data Entered)*

20. Abstract (Cont'd):

these radical species were obtained by assuming overall first-order kinetics. The experimentally determined temperatures and species concentrations are compared with thermochemical equilibrium calculations.

SUMMARY

A simple experimental technique which is non-intrusive and spatially precise has been described. It can (1) profile absolute concentrations of a variety of species down to about the 1% level in a flame environment, (2) profile the temperature with an accuracy of about ±4%, and (3) profile the relative concentrations of some flame intermediate radical species. Estimates can also be made for the absolute concentration of these flame intermediates. The major sources of uncertainty in the concentrations obtained are the precise differences, if any, between the laser frequency and the molecular transition frequency and the quench rates. Since the accuracy of these two quantities may be improved by future studies, the method of data analysis has been discussed in detail in order to facilitate updating the present concentration results. Loss rates for CN, NCO, OH and NH have also been computed and these values can provide a check on the predictions of multispecies kinetic mechanisms which attempt to model flame chemistry.

In addition to the molecules discussed here, the application of this technique to rich flames allows concentration profiles of CO, H_2 and C_2 to be obtained. Raman signals of both CO_2 and N_2O are of sufficient intensity to permit profiling; however, a more detailed spectroscopic model is required to extract densities as a function of temperature.

TABLE OF CONTENTS

LIST OF FIGURES

I. INTRODUCTION

In recent years there has been much progress in using laser based probes for investigating detailed combustion processes.[1,2] We report here a simple experiment which provides detailed spatially precise information on steady state atmospheric pressure flames from the various Raman and fluorescence signals that are observed. Spontaneous Raman spectroscopy has become an accepted method for making non-intrusive temperature and major species concentration measurements in relatively clean flames.[3-6] For studying trace flame species occurring typically at less than one percent concentration, Raman signals are, in general, too small to be observed above the background signals, thus other techniques such as absorption and/or fluorescence spectroscopy are used. Bechtel[7] has combined Raman and fluorescence techniques to obtain temperature and species concentration profiles through the reaction zone of premixed laminar methane-air flames. The profiled species were CH_4, CO_2, CO, O_2, N_2, H_2 and OH. More recently, Cattolica, et al.[8] have profiled NH, OH and NO and temperature in the reaction zone and burnt gas regions of a premixed laminar hydrogen-nitrous oxide flame using fluorescence, absorption and thermocouple measurements. The emphasis of this paper is the explanation and demonstration of the technique rather than

---

[1] *D. Crosley, ed., Laser Probes for Combustion Chemistry, ACS Symposium Series 134, 1980.*

[2] *A. C. Eckbreth, "Recent Advances in Laser Diagnostics for Temperature and Species Concentration in Combustion," Proceedings, Eighteenth International Symposium on Combustion, Combustion Institute, Pittsburgh, p.1471,1981.*

[3] *D. A. Stephenson, "Non-Intrusive Profiles of Atmospheric Premixed Hydrocarbon-Air Flames," Proceedings, Seventeenth International Symposium on Combustion, Combustion Institute, Pittsburgh, p.993,1978.*

[4] *J. A. Vanderhoff, R. A. Beyer and A. J. Kotlar, "Raman Spectroscopy of Premixed CH_4/N_2O and H_2/N_2O Flames," Proceedings, First International Specialists Meeting of the Combustion Institute, Bordeaux, France, Vol.2, Combustion Institute, Pittsburgh, 1981, p. 551.*

[5] *M. Lapp, "Flame Temperatures from Vibrational Raman Scattering," Laser Raman Gas Diagnostics, M. Lapp and C. M. Penney, eds., Plenum Press, New York and London, p.107,1974.*

[6] *M. Bridoux, M. Crunelle-Cras, F. Grase and M. Delhaye, "Use of Multichannel Pulsed Raman Spectroscopy as a Diagnostic Technique in Flames," Combust. Flame, Vol. 36, p. 109, 1979.*

[7] *J. H. Bechtel "Laser Probes of Premixed Laminar Methane-Air Flames and Comparison with Theory," Laser Probes for Combustion Chemistry, D. Crosley, ed., ACS Symposium Series 134, p. 85, 1980.*

[8] *R. Cattolica, M. Smooke and A. Dean, "A Hydrogen-Nitrous Oxide Flame Study," Fall Meeting of the Western States Section of the Combustion Institute, Sandia National Laboratories, Livermore, CA, Paper WSS/CI p. 82-95, 1982.*

addressing in detail the actual chemistry occurring in a flame. In the present study, a lean methane-nitrous oxide flame in which the fuel-oxidizer premixed gas is diluted with nitrogen is probed and temperature and species profiles for CH_4, N_2, H_2O, CN, NCO, OH and NH are obtained. We have previously reported excitation of C_2[9], CN,[9,10] and NCO[11] in a flame with prism selected lines of ion lasers; however, this is the first report of excitation of NH and OH in this manner. The primary reason for selecting this flame system for investigation is to provide an easily managed source of various flame species which can be probed with the Raman and fluorescence techniques.

II. EXPERIMENT

A schematic diagram of the experiment is shown in Figure 1. Either an argon or krypton ion laser, eight watts and three watts respectively (all lines) with prism selection of wavelengths, is used as the excitation source. The laser cavities have been extended by uv and visible mirror sets of radii of curvature 1.0 and 0.3 m similar to the intracavity experiment described by Hercher et al.[12] This arrangement results in an intracavity beam waist of about 100 μm diameter and a laser power enhancement of one to two orders of magnitude depending on the laser wavelength used. The scattered light is imaged onto 100 μm entrance slits of a 0.25 m spectrometer with two convex quartz lenses. These are an f/1.0 collector lens with a 7.6 cm. focal length and an f/1.7 focussing lens of 12.7 cm. focal length. The detected light is from a sampled volume which approximates a cylinder of 100 μm diameter and 2 mm in length. An optical multichannel analyzer system (OMAI) incorporating a silicon intensified target vidicon tube is used to detect the dispersed light. The spectrometer has two gratings which are switch selectable. For observing radiation wavelengths longer than 4500Å, the 1180 grooves/mm grating was used. Approximately 400Å of the spectrum could be observed at one time with this grating. The entrance slits of the spectrometer provide a resolution, FWHM, of approximately 12 cm^{-1}. Two memories of the OMA allow for summation of scans and subsequent subtraction of background (laser off) to obtain the signal due to Raman scattering or laser

---

[9] *J. A. Vanderhoff, R. A. Beyer, A. J. Kotlar and W. R. Anderson, "Ar^+ Laser - Excited Fluorescence of C_2 and CN Produced in a Flame,"* Combust. Flame *Vol. 49, p. 197, 1983.*

[10] *J. A. Vanderhoff, R. A. Beyer, A. J. Kotlar and W. R. Anderson, "Kr^+ and Ar^+ Laser - Excited Fluorescence of CN in a Flame,"* App. Opt. *Vol. 22, p. 1976, 1983.*

[11] *W. R. Anderson, J. A. Vanderhoff, A. J. Kotlar, M. A. Dewilde and R. A. Beyer, "Intracavity Laser Excitation of NCO Fluorescence in an Atmospheric Pressure Flame,"* J. Chem Phys. *Vol. 77, p. 1677, 1982. K. N. Wong, W. R. Anderson, A. J. Kotlar, and J. A. Vanderhoff, to be published.*

[12] *M. Hercher, W. Mueller, S. Klainer, R. F. Adamowicz, R. E. Meyers and S. E. Schwartz, "An Efficient Intracavity Laser Raman Spectrometer,"* Appl. Spectros. *Vol. 32, p. 298, 1978.*

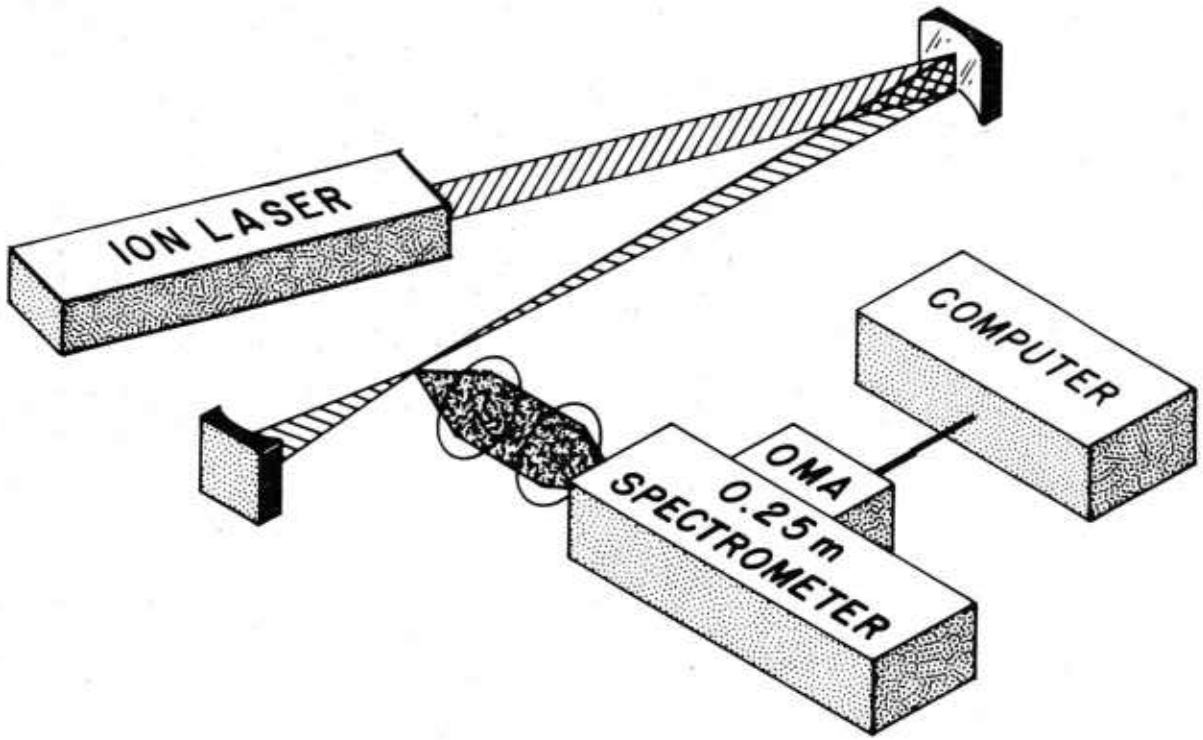

Figure 1. Schematic diagram of apparatus used for Raman and flourescence measurements

induced fluorescence. In many cases the number of scans summed exceeds full scale of the OMA memory. Thus, a roll over occurs. The background signal is similarly large causing significant truncation errors when the background is subtracted. This problem is avoided by digitization and storage of the OMA signals in a PDP 11/34 computer. A description of the procedure and software for interfacing the computer with the OMA is discussed elsewhere.[13]

Accumulation times for the data presented here are two minutes for each full Raman spectrum and one minute for each fluorescence spectrum. As a rough estimate of the sensitivity of the experiment we could obtain about 3×10^4 counts/sec for the Stokes Q-branch signal of nitrogen in room air using about 50 watts of 4880Å laser radiation. Both the Raman and fluoresence signals from the reaction zone of the flame could be readily observed real time on a display oscilloscope. The discovery of these unexpected fluorescence signals stemmed from this capability.

To obtain a temperature measurement only the spectral shapes of the Raman signals are required; however, for determination of concentrations the laser power and a calibration factor are also required. A small fraction of laser light transmitted by one of the high reflectivity cavity mirrors is monitored with a thermopile to determine a relative average laser power during data acquisition. Calibration factors for N_2 and H_2O are obtained from ambient air. A calibration factor for CH_4 is obtained by flowing 100% CH_4 unignited through the burner at ambient temperature.

A lean premixed flame of methane and nitrous oxide diluted with nitrogen operating at atmospheric pressure was supported on an open channel curved knife-edge burner that has been previously described.[14] The gas flows to this burner are controlled with various sintered plug flow restricters and a pressure gauge monitor. Calibration of the flow rates are obtained from a wet test meter or, for the slower flow rates from a traveling soap bubble method. The flame conditions for the data reported here are an equivalence ratio of 0.83 diluted by 52% nitrogen. An advantage of this burner design is that it allows probing through the entire reaction zone of a flame. In the previously published work we have operated the burner in the horizontal position, that is, the flame can be directly viewed end on by the detection optics. Here, the long dimension of the entrance slits was aligned with the long dimension of the channel. For the present work, the burner is rotated 90° to a vertical position where the burner throat points up. Thus, the flame is viewed from the side. The orientation was used to minimize possible self absorption effects for OH in the fluorescence results. Variation of the burner position is accomplished with a micrometer drive screw and the position is monitored with a dial gauge which reads directly to 25.4 μm. The flow rates of the gases are adjusted such that most of the reaction zone can be directly viewed from the side. This view is not complete enough to observe the initial fuel and oxidizer gases at ambient temperature but the position where radical species form is directly observable.

---

[13] *M. A. Dewilde, Ballistic Research Laboratory Report to be published.*

[14] *R. A. Beyer and M. A. Dewilde, "Simple Burner for Laser Probing of Flames," Rev. Sci. Instr., Vol. 53, p. 103, 1982.*

Insertion of this burner into the laser beam at the intracavity focus results in a minimal decrease in laser power for most regions of the flame. Nonetheless, there is one position in the flame which causes the laser power to drop by a factor of two or more! At this position, maximum laser beam deflection occurs due to changes in the index of refraction resulting from the steep temperature gradient. Weinberg[15] has discussed this effect in detail and has determined the maximum beam deflection occurs between 1.5 and 2.0 T_i, where T_i is initial temperature, depending upon the actual temperature dependence of the termal conductivity and specific heat.

An approximate calculation was made to determine the displacement in laser beam position, which is analogous to an error in burner position. The value obtained was 12 μm. An experimental determination of this displacement was also performed in the following way. The small amount of light that is transmitted through the laser end mirror was used to produce a spot on a distant target. Movement of the flame through the laser beam focus resulted in a measurable movement of the laser beam spot on the target. A simple geometrical calculation indicated that a maximum displacement of about 17 μm occurred. This value is a factor of five smaller than the laser beam waist and thus considered a negligible correction to burner position. This beam deflection can, however, cause appreciable displacement for larger burners. For instance, Cattolica,[8] et al. found that they could not obtain any measurements closer than 0.4 mm from the burner surface in their H_2/N_2O flame studies. One advantage of this maximum beam deflection point is that it provides a sensitive reference for position in the flame.

III. RAMAN SPECTROSCOPY

Both the 4880Å line of an Ar^+ laser and the 3507Å line of a Kr^+ laser have been used to generate Raman spectra. Most of the Raman data is derived from the most frequently used ion laser line, 4880Å; but a change of lasers was required to obtain fluorescence data for OH and NH. Some Raman spectra from the 3507Å line were obtained for comparison.

IV. TEMPERATURE

Temperature measurements through the flame were determined from fits of the experimentally measured Q-branch rotational-vibrational Stokes Raman spectra for the nitrogen molecule. An example of the experimental data and corresponding computer fit is shown in Figure 2. Here, the experimental spectral resolution is sufficient to clearly identify the vibrational bands but the rotational lines appear only as a spread of each vibrational band. A multivariate least squares Raman fitting program has been developed which computes synthetic spectra and compares these spectra with the experimental data in a least squares sense. The resulting output is a best fit to the temperature and concentration for nitrogen together with one standard

---

[15] *F. J. Weinberg, Optics of Flames, Butterworth, Inc., Washington, D.C., p. 7, 1963.*

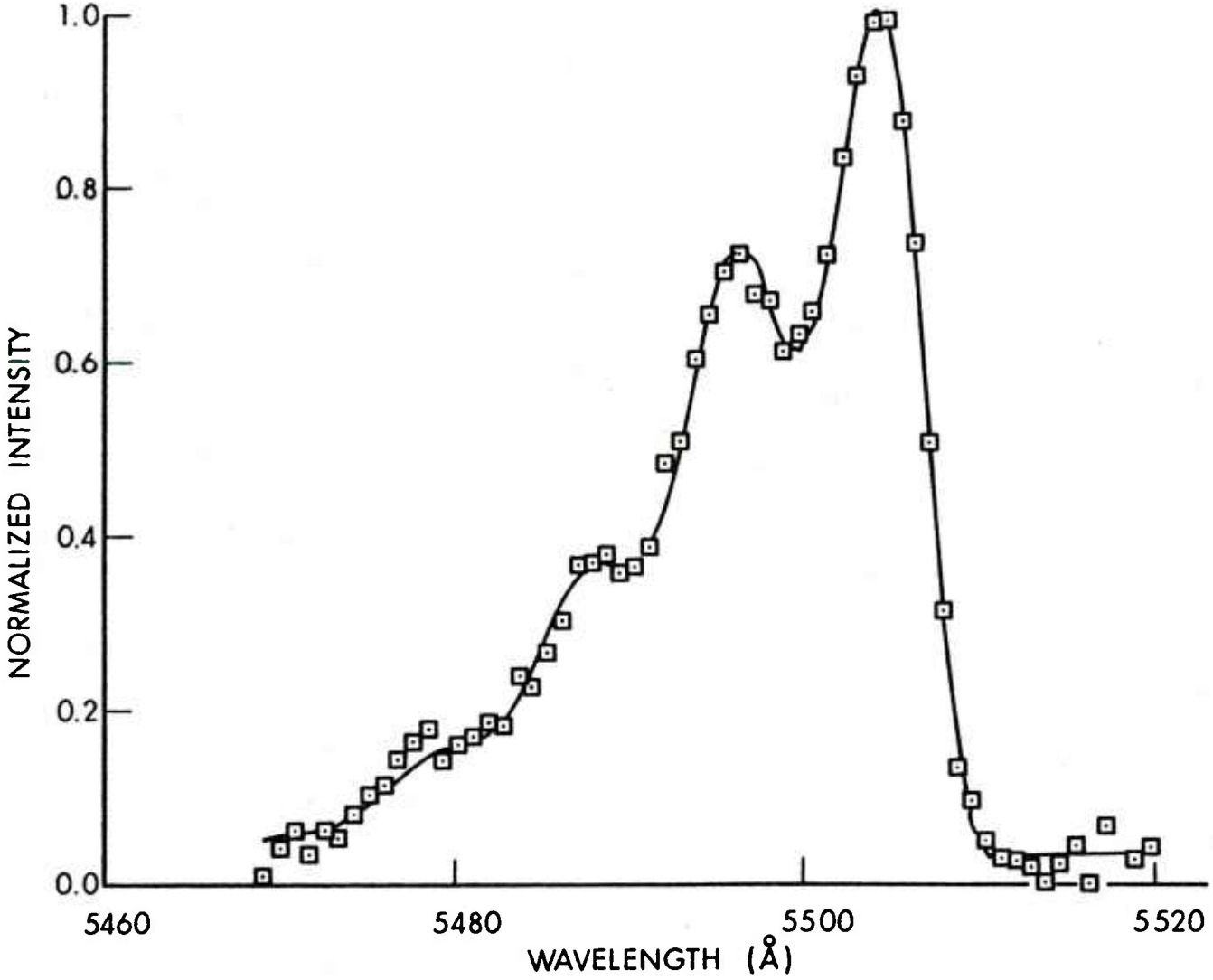

Figure 2. N_2 stokes Q-branch Raman data (⊡) and computer fit (-) in the burnt gas region of a CH_4/N_2O flame

deviation error. Details of this fitting program are discussed elsewhere.[16] For temperatures above ~ 1000K, the standard deviation in temperature is about 1%. Below ~ 1000K, there is negligible population in the hot bands of N_2, and thus, the temperature fit relies on fitting only the rotational line contour of the ground vibrational state. This results in a larger uncertainty.

V. CONCENTRATION

As mentioned in the previous section concentration values for N_2 are obtained from the fitting program. These values are not normalized and must be adjusted by the relationship

$$N = N_o\left(\frac{T}{T_o}\right)\left(\frac{\phi_o}{\phi}\right)\left(\frac{W}{W_o}\right) \quad , \tag{1}$$

where N, T, ϕ and W refer to density, temperature, laser flux and a weighting factor, respectively. The subscript o refers to the calibration conditions and the weighting factor is related to the integral of the Raman signal. For N_2, this weighting factor is obtained from the fitting program which takes into account the scaling of the spectrum as $(v+1)/Q$. Here, v is the initial vibrational quantum number and Q is the partition function. This term multiplied by a rotational line strength, the Boltzmann factor, and W relates the fraction of scattering species in the appropriate initial quantum states to the observed signal. The concentrations of H_2O and CH_4 were obtained directly from the integral of the Raman signal without further correction. This approximation is valid when $h\nu_1 > kT$, where h is Planck's constant, ν_1 is the lowest vibrational band frequency and k is Boltzmann's constant.

A plot showing the temperature and concentrations of N_2, H_2O and CH_4 as a function of burner position is given in Figure 3. Points represented by blacked in symbols refer to data resulting from the 4880Å laser line, open symbols refer to the 3507Å laser line. Laser induced fluorescences from the 3507Å line precluded obtaining any Raman measurements in the reaction zone of this flame. As a comparison, the NASA - Lewis[17] thermochemical equilibrium computer code was used to calculate equilibrium concentrations and an adiabatic flame temperature of 2399 K. This temperature is denoted by the arrow on the right ordinate and compares well with the maximum experimentally determined temperature indicating that there is negligible heat loss to the burner. Equilibrium mole fractions of 0.756 for N_2 and 0.129 for H_2O agree with the experimentally determined values in the burnt gas region of the flame. These values are shown by arrows on the left ordinate. Initial mole fractions of 0.082 for CH_4 and 0.52 for N_2 are determined from the flow rate calibrations. These values are also shown on the left ordinate with arrows.

---

[16] *A. J. Kotlar, Ballistic Research Laboratory Report, to be published.*

[17] *R. A. Svehla and B. J. McBride, "Fortran IV Computer Program for Calculation of Thermodynamic and Transport Properties of Complex Chemical Systems," NASA, TND - 7056, 1973.*

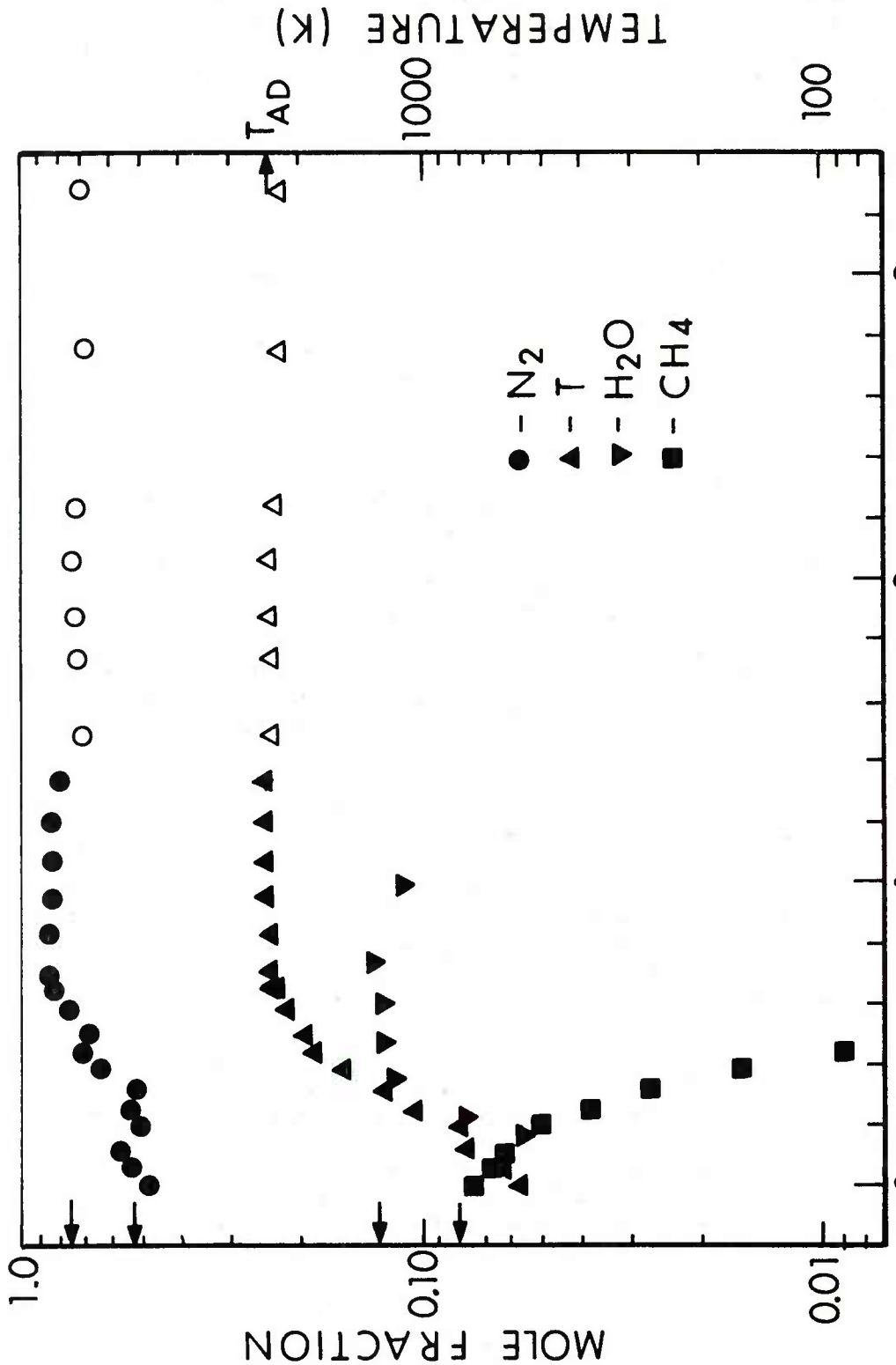

Figure 3. Temperature and concentration profiles for N_2, H_2O and CH_4 through the flame zone of a CH_4/N_2O flame obtained from Raman data

Mole fractions of CO and H_2 were too small to be easily measured for this lean flame. However, for richer flames, these species occur in larger concentrations and can be measured by this technique. There is ample Raman signal from CO_2 and N_2O but the criterion $h\nu_1 > kT$ is not met and a simple integration to determine mole fraction is not valid. Thus, these concentrations values have not been determined.*

The results of Figure 3 show that most of the reaction zone has been probed and the measurements continue well into the burnt gas region of the flame. Maximum laser beam deflection occurs at a position just prior to the first measurement point which is at a temperature of 560 K. A comparison of the Raman data from the 3507Å and 4880Å laser lines demonstrate the reproducibility of the results since these data involved operating the burner on different days and also a change of lasers with the associated realignment. Comparing these data sets with each other and with the thermochemical equilibrium values should be a representative estimate of total error which turns out to be about ±10% for concentration and ±4% for temperature.

VI. FLUORESCENCE SPECTROSCOPY

We have previously reported the transitions used to excite CN[9,10] and NCO[11] using prism selected lines of ion lasers. These assignments are summarized in Table 1. Excitation of OH and NH with the 3507Å line of a krypton ion laser has not been previously reported; thus, the method used to assign these transitions will be discussed here. These transitions are also listed on Table 1.

---

*The temperature dependent Raman spectroscopy for CO_2 has been reported; R. J. Blint, J. H. Bechtel, and D. A. Stephenson, "Carbon Dioxide Concentration and Temperature in Flames by Raman Spectroscopy," J. Quant. Spectrosc. Radiat. Transfer, Vol. 23, P. 89, 1980. However this approach has not been implemented. To our knowledge no one has yet reported a similar approach for the N_2O molecule.

TABLE 1. Ar^+ AND Kr^+ LASER LINES USED TO PUMP FLAME RADICAL SPECIES AND THE PROBABLE PUMPING TRANSITIONS. ALSO THE QUENCH RATES, ABSORPTION COEFFICIENTS AND VIBRATIONAL BAND EMISSION COEFFICIENTS USED TO ESTIMATE ABSOLUTE CONCENTRATIONS FROM THE FLUORESCENCE DATA ARE LISTED.

Species	Laser Wavelength (Å)	Transition Wavelength (Å)	Transition	Quench Rate (sec^{-1})	Emission Coefficient A_{21} (sec^{-1})	Absorption Coefficient B_{12} cm^2-B_z erg sec
CN	4545.04	4545.051	$B^2\Sigma^+ \leftarrow X^2\Sigma^+$ (1,3) R (20)	1×10^9	1.10×10^7	4.24×10^{16}
NCO	4657.95		$A^2\Sigma^+ (0,0^0,0) \leftarrow X^2\pi (1,0^1,0)$ Q_2 (31)	1×10^9	1.57×10^6	1.06×10^{17}
OH	3507.42	3507.46	$A^2\Sigma^+ \leftarrow X^2\pi$ (0,1) Q_1 (19)	1×10^9	9.82×10^5	4.55×10^{14}
NH	3507.42		$A^3\pi \leftarrow X_1^3\Sigma^-$ (0,0) , N' = 21			

TABLE 2. A-X OH BAND SYSTEM TRANSITIONS AND RQ AND QP SPLITTINGS. ALL VALUES ARE GIVEN IN Å (WAVELENGTH IN STANDARD AIR). SPLITTINGS FOR F_2 EMISSION ARE NEARLY THE SAME AS THESE GIVEN FOR EQUAL N VALUES

Excited State N'	(0,0) A-X				(0,1) A-X			
	Q_1	Q_2	R_1Q_1	Q_1P_1	Q_1	$Q_{P_{21}}$	Q_2	$Q_{R_{12}}$
17	3130.6	3133.2	58.3	61.2	3498.18	3498.63	3501.66	3501.10
18	3136.6	3139.2	61.5	64.4	3502.66	3503.14	3505.92	3505.44
19	3143.0	3145.5	64.6	67.5	3507.46	3507.96	3510.63	3510.12
20	3149.8	3152.3	67.8	70.6	3512.60	3513.12	3515.68	3515.16
Observed	3141.5		64.1	69.1		3507.42		

VII. OH

Both an emission and a fluorescence spectrum for OH is shown on Figure 4. There is sufficient resolution in the emission spectrum to identify six prominent heads by which a wavelength scale can be assigned to within ± 2Å. This provides a wavelength scale for the fluorescence spectrum from which the wavelength of the Q-branch emission line resulting from the pumped level can be determined. The wavelength spacing of the RQ and QP splittings are also determined. In Table 2, these observed values are compared with values calculated after refitting the data of Diecke and Crosswhite.[18] A comparison of the laser wavelength with some (0,1) Q-branch transitions is also given in this table. The only transition consistent with the observed data is (0,1) Q_1 (19).

VIII. NH

An emission and fluorescence spectrum for NH are shown on Figure 5. Three Q-head features can be identified in the emission spectrum and a wavelength scale thus established for the fluorescence spectrum. These features are relatively close together and not as distinct as in the OH emission spectrum. Consequently, there is more uncertainty (~±5Å) for portions of the wavelength scale far removed from these emission features. R, Q, and P branches can be observed in the fluorescence spectrum of NH and again the wavelength of the excited Q-branch together with the spacing of the RQ and QP splittings can be assigned. These values are given in Table 3, together with the data of Dixon.[19] An approximate value for the excited N' can be determined from this table. There is no sharp excitation peak in the P-branch, and the Q-branch lines are very close together so it was initially thought that the best estimate of N' would come from the RQ splitting. However, when examining the R-branch region under higher resolution, this apparent peak turned out to be an R-branch head, not a definable excited line. Thus, pinpointing the value for N' from the RQ splitting was not possible. Only an approximate value of $N'=21\pm2$ is derived from the QP splitting as shown in the Table.

As an alternative, the appropriate N' can be determined from the energy of the laser excitation line. We have not found any existing data or calculations for NH (0,0) A-X transitions in this region. The data of Funke,[20] as reassigned by Dixon,[19] together with the $X^3\Sigma^-$ state constants of

---

[18] *G. H. Diecke and H. M. Crosswhite, "The Ultraviolet Bands of OH Fundamental Data," J. Quant. Spectrosc. Radiat. Transfer, Vol. 2, p. 97, 1962.*

[19] *R.N. Dixon, "The 0-0 and 1-0 Bands of the $A^3\pi - X^3\Sigma^-$ Systems of NH," Can. J. Phys., Vol. 37, p. 1171, 1959.*

[20] *(a) G.W. Funke, "Die NH-Banden bei λ 3360," Z. Physik, Vol. 96, p. 787, 1935. (b) G.W. Funke, "Das Absorptionsspektrum des NH," Z. Physik, Vol. 101, p. 104, 1936.*

Murai and Shimachi,[21] can be used to obtain estimates of transitions which could produce NH excitation. The only reasonable possibilities are the O-branch transitions near $N'' = 21$. The calculation is performed by first noting that each O-branch transition will excite a $^3\Pi$ level which also connects to an allowed main Q-branch transition. These O and Q branch lines have different ground state levels and the appropriate term energy pairs were calculated using the equations of Murai and Shimachi. The difference of these term energies was subtracted from the main Q-branch energy. The best agreement between the laser excitation line and possible pumping transitions are for O-branch transitions with $N' = 19$. The wavelength of these transitions are estimated as 3507.11, 3507.33 and 3507.35 Å for $^{O}P_{23}(21)$, $^{O}P_{12}(21)$ and $^{O}Q_{13}(21)$, respectively. Formulas of Reference 21 were used because the second order centrifugal distortion term is included. This term is important when extrapolating to high N'' values as is illustrated by comparing the calculation with that obtained when using the formulas of Reference 19 without the second order centrifugal distortion term. The resulting estimates for the O-branch triplet are ~ 0.5Å higher than the laser excitation line, which would result in no excitation at all.

While the quality of the present calculations are not precise enough to determine which line of the O-branch triplet is being pumped, it can be clearly determined that $N'' = 21$ since the next set of triplets in the sequence ($N'' = 20$ and 22) are estimated to be ~ 60 cm^{-1} away from the laser line. Efforts to refine the calculations using a proper Hamiltonion to fit the (0,0) band data and then extrapolate to $N'' = 21$ are underway.

Given that an O-branch transition in NH is being pumped, it becomes clear why there are no sharp peaks from the excited state in the R and P branches. Due to the selection rules on parity for the $A^3\pi$ state of NH the component of the lambda doublet which gives rise to the R and P branches cannot be directly excited by an O-branch transition, while the component which gives rise to the Q-branch can. The smeared out excitation that does appear for the R and P branches apparently arises from collisional energy transfer between opposite parity levels which has a modest N' retention. This retention allows us to rule out the possibility that a P-branch transition of extremely high N'' is being pumped. Using the result that $N'' = 21$, a relative concentration profile may be determined by assuming a Boltzmann population distribution. There are several other peaks arising in the fluorescence spectrum shown in Figure 5. A peak at about 3355Å is in the appropriate position for the anti-Stokes Raman Q-branch signal for N_2O. The peak at about 3370Å is fluorescence from the Q-head of the (1,1) band of NH. It is not clear how this band is being excited. Possibilities are vibrational up transfer in the excited state or that the laser line overlaps more than one NH transition.

---

[21] *T. Murai and M. Shimachi, "Rotational Distortions of $^3\pi$ States Applied to the NH Molecule," Science of Light, Vol. 15, p. 48, 1966.*

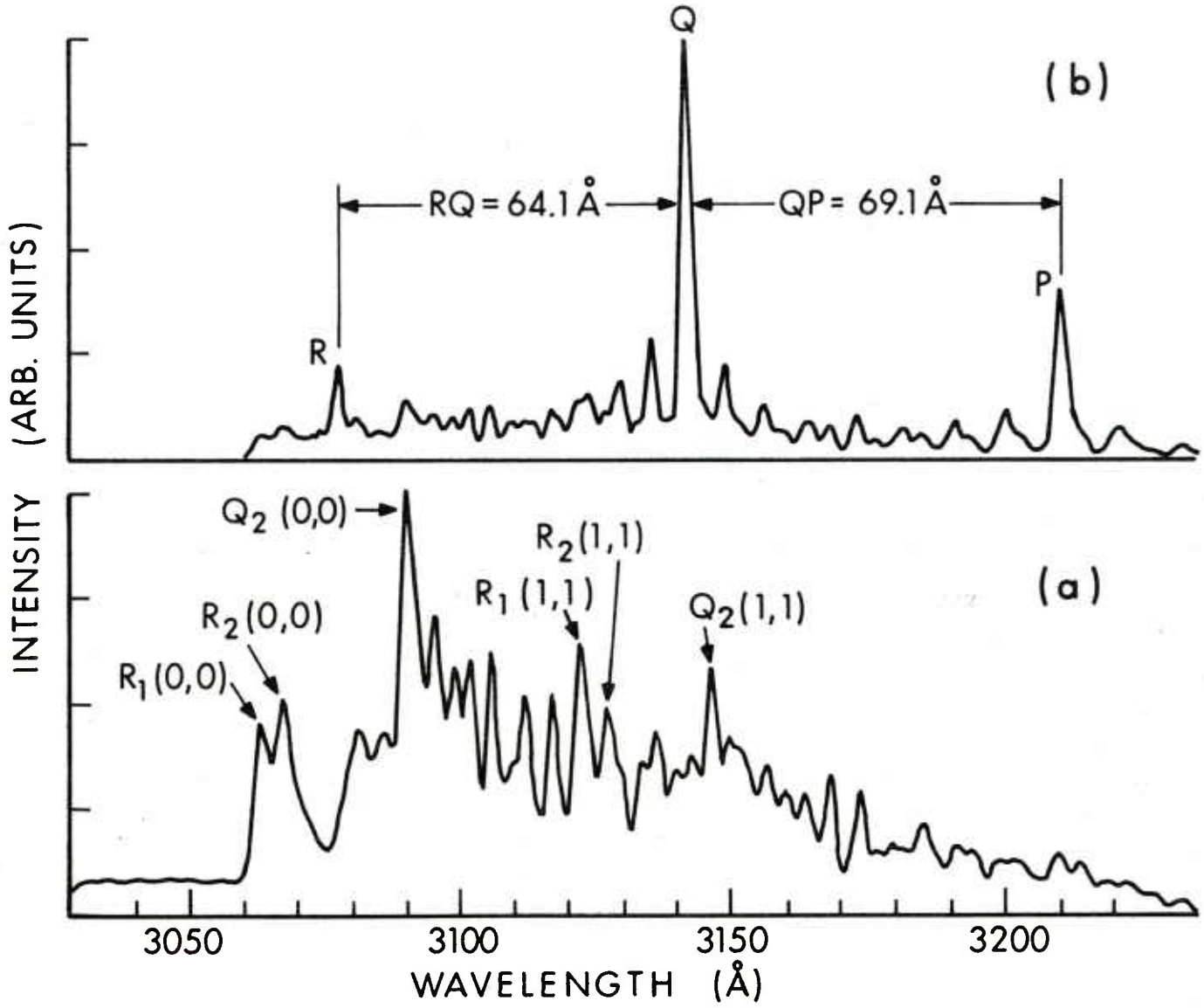

Figure 4. (a) OH emission spectrum and (b) fluorescence spectrum from the reaction zone of a CH_4/N_2O flame. The laser excitation wavelength is 3507.42Å

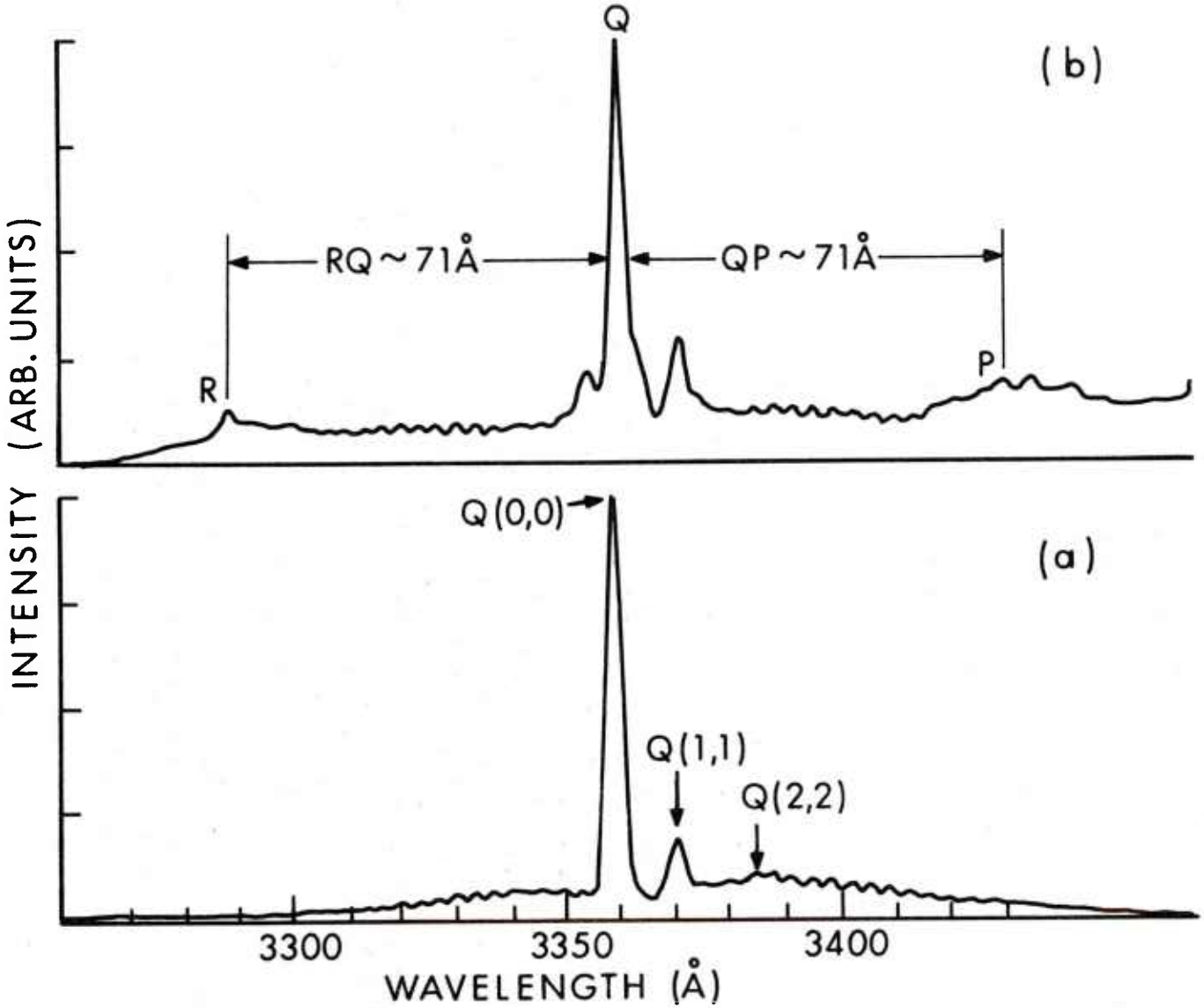

Figure 5. (a) NH emission spectrum and (b) fluorescence spectrum from the reaction zone of a CH_4/N_2O flame. The laser excitation wavelength is 3507.42Å

TABLE 3. (0,0) A-X NH BAND SYSTEM TRANSITIONS AND THE RQ AND QP SPLITTINGS

Excited State N'	(0,0) A - X Q_1	Q_2	Q_3	R_1Q_1	Q_1P_1
19	3362.2	3362.3	3361.8	67.5	64.9
20	3362.7	3362.7	3362.4	70.2	67.7
21	3363.3	3363.4	3363.0	72.8	70.5
22	3364.0	3364.0	3363.6	75.4	73.1
23	3364.6	3364.7	3364.3	77.8	75.7
Observed		3361^{+2}_{-1}		71±5	71±10

IX. CONCENTRATION PROFILES

Relative concentration profiles for CN, NCO, OH and NH can be determined from the fluorescence intensity and temperature data if a Boltzmann population distribution and a constant quench rate (Q) is assumed for the different positions sampled in the flame. In the latter parts of the reaction zone and the burnt gas region where the temperature has approached its maximum value and the fuel and oxidizer have been converted to final products, the quench rate should be constant; however, in the early stages of the reaction zone where initial products are changing to final products, the quench rate might be expected to vary. Nonetheless, previous investigations[22,23] have shown that the quench rate for OH is essentially constant through the reaction zones of propane-oxygen and methane-air flames. To change the fluorescence intensity data to relative concentration, normalization by means of Eq. 1 is used. In addition, these values then need to be adjusted by the Boltzmann population distribution to reflect the number of molecules in the state which is pumped.

Before plotting the relative concentration values as a function of burner position rough estimates of the absolute concentrations can be calculated by the following procedure. Assuming the laser lines and molecular transitions are Doppler broadened, a solution for the transmission of the laser light through a sample is:

---

[22] *J. J. Cottereau and K. Stepowski, "Laser Induced Fluorescence Spectroscopy Applied to the Hydroxal Radical in Flames," Laser Probes for Combustion Chemistry, D. Crosley, ed., ACS Symposium Series 134, p. 131, 1980.*

[23] *J. H. Bechtel and R. E. Teets, "Hydroxal and Its Concentration Profile in Methane-Air Flames," Appl. Opt., Vol.18, P. 4138, 1979.*

$$\frac{P}{P_o} = 1 - \left(\frac{h\nu_o L}{c}\right) B_{12} N_g \left[\frac{A\alpha}{\pi(A+\alpha)}\right]^{1/2} \exp\left[\left(\frac{-A\alpha}{A+\alpha}\right)(\nu_1-\nu_o)^2\right] , \qquad (2)$$

where P and P_o are the transmitted and incident laser powers, respectively, h is Planck's constant, ν_o is the molecular transition line center frequency, L is the length of the sample in the direction of the laser beam, c is the speed of light, B_{12} is the Einstein absorption coefficient for the pumping transition, N_g is the density of the ground level being pumped, ν_1 is the laser line center frequency, and A and α are related to the line shapes

$$A = 4 \ln 2/\Delta\nu_o^2 , \qquad \alpha = 4 \ln 2/\Delta\nu_1^2, \qquad (3)$$

where $\Delta\nu_o$ and $\Delta\nu_1$ are the molecular transition and laser linewidths (FWHM), respectively. Generally, atmospheric pressure flames have quench rates much larger than spontaneous emission rates from the excited state. Experimentally it has been shown that the transitions are not saturated. For these reasons stimulated and spontaneous emission can be ignored. Thus, the fluorescence emission per unit time F from the probed volume of length L is given by

$$F = \frac{P_o [1 - (P/P_o)]}{h\nu_o} \quad \frac{A_{21}}{Q} , \qquad (4)$$

where A_{21} is the Einstein emission coefficient for the observed vibrational band. The integrated signal under the vibrational band seen by the detector is

$$S = \frac{F\Omega\varepsilon_\lambda}{4\pi} , \qquad (5)$$

where Ω is the solid angle subtended by the collection optics and ε_λ is the wavelength-dependent transmission efficiency of the detector system. Eqs. (2)-(5) provide a relation between the fluorescence signal S and the density N_g. The total density N_t is obtained from

$$N_t = N_g \Phi / g_J \exp(-E_J/kT) , \qquad (6)$$

where Φ is the partition function for the molecule at the measured flame temperature and g_J and E_J are the degeneracy and energy of the pumped state, respectively.

The quantity $\Omega e_\lambda L P_o$ is experimentally determined for the detection system from the Raman-Stokes rotational-vibrational Q-branch signal of N_2 in ambient air. The Stokes power P_s is given by

$$P_s = \sigma_1 \left(\frac{\nu_1}{\nu_s}\right) \Omega\varepsilon_\lambda L P_o \qquad (7)$$

where σ_1 is the Raman scattering cross section at the laser frequency, and ν_s is the Stokes frequency. Calibrations are performed using the same laser frequency as that used for the fluorescence excitation. Nonetheless, the Stokes Raman signals do not appear at the same frequencies as the fluorescence signal, necessitating the use of a factor obtained from the spectral response graph for the OMA detector. The Raman scattering cross sections[24] at the various laser wavelengths were obtained by adjusting the scattering cross section at 4880Å by the factor $(\nu_{4880Å}/\nu_1)^4$. Calculations to convert the fluorescence intensities to absolute concentrations were performed at the peak of the radical concentration where the temperature is 2400K.

The temperature and concentration profiles for CN, NCO, OH and NH as a function of burner position are shown in Figure 6. An example of some of the raw laser excited fluorescence data used to obtain the concentration profile for NCO is shown in Figure 7. Sixteen fluorescence spectra for different burner positions are displayed. The NCO fluorescence starts to rise sharply at about 1800K and exists over about a 1 mm extent in the flame zone. Figure 7 demonstrates that NCO is a sharply peaked, short lived radical species. Previously, we have discussed extracting concentration profiles from the laser excited fluorescence of CN[9] and NCO.[11] The values used for the quench rate, emission coefficients, and absorption coefficients are summarized in Table 1. In this paper, the laser wavelength values were obtained from Bridges and Chester.[25] These values are also listed in Table 1. The calculated peak concentration for CN is 6.3×10^{13} molecules/cm^3. For NCO, the transition wavelength is assumed to be the same as the laser wavelength which maximizes the value of the exponential in Eq. 2. This results in a minimum value of 3.4×10^{14} molecules/cm^3. The fluorescence data is converted to relative concentrations and normalized to these peak concentration values. Figure 6 shows these results. The OH concentration has also been calculated in this manner and the resulting minimum value for the concentration is 1.7×10^{16} molecules/cm^3. Since the concentration is extremely sensitive to the exponential term, it was decided that a better estimate of the absolute concentration would be that computed from the NASA-Lewis thermochemical equilibrium using our flame conditions. This concentration is computed to be 2.2×10^{16} molecules/cm^3 and is assigned to the data point highest up in the flame, 4.54 mm. This point is necessarily the most representative of equilibrium conditions since it is the furtherest from the reaction zone. All of the other data are normalized to this value resulting in a peak concentration of 3.9×10^{16} molecules/cm^3. All of the observed radicals, except OH, have decayed to negligible values; the major burnt gas species and the temperature have reached equilibrium as well. Unfortunately, equilibrium conditions may not have been reached by OH, which together with diffusive losses presents additional uncertainty in assigning the absolute concentration in this manner.

---

[24] *A. C. Eckbreth, P. A. Bonczyk and J. F. Verdieck, "Laser Raman and Fluorescence Techniques for Practical Combustion Diagnostics,"* Appl. Spectros. Rev., *Vol. 13, P.52, 1978.*

[25] *W. B. Bridges and A. N. Chester, "Visible and uv Laser Oscillation at 118 Wavelengths in Ionized Neon Argon, Krypton, Xenon, Oxygen and other Gases,"* Appl. Optics, *Vol. 4, P. 573, 1965.*

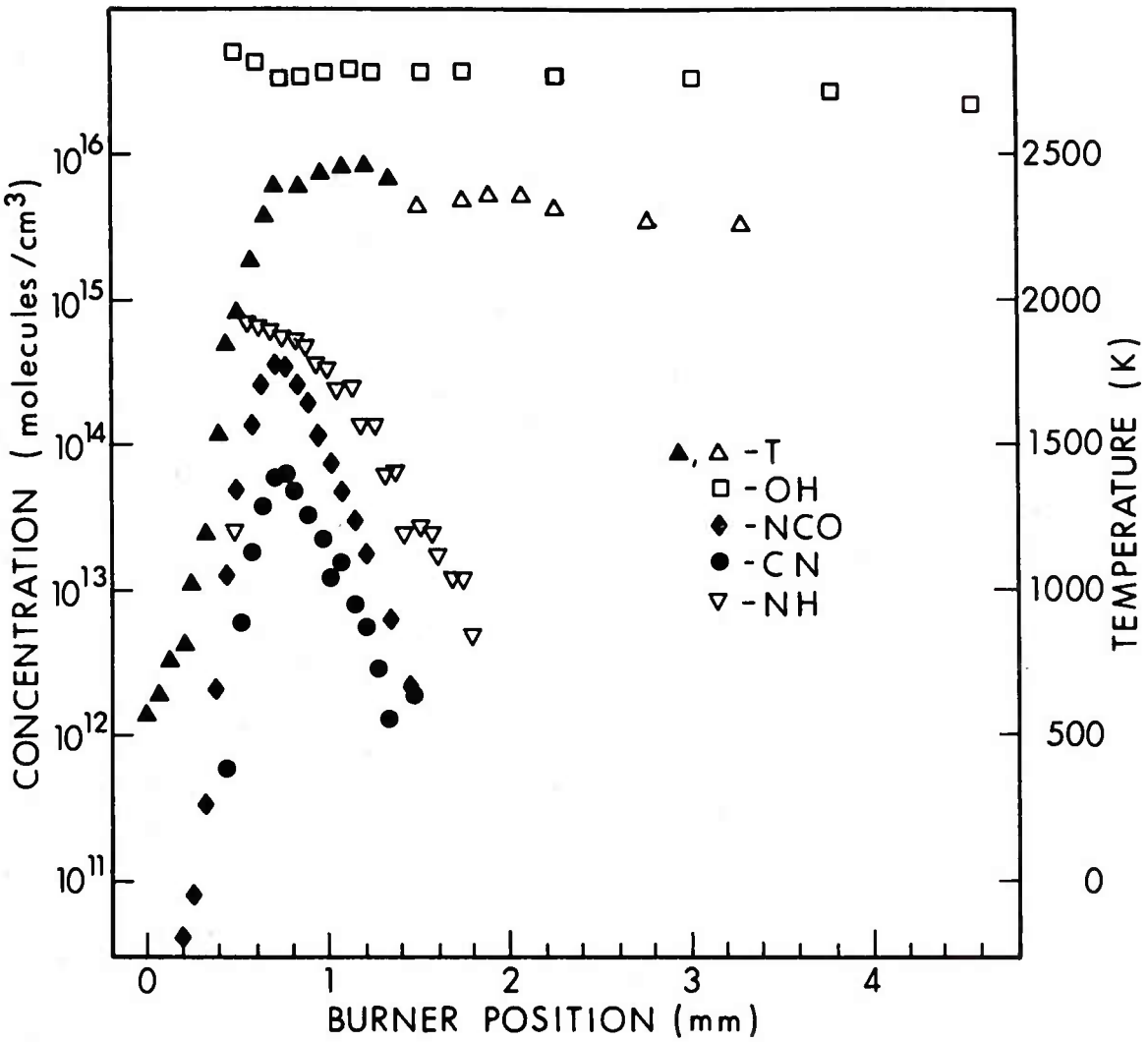

Figure 6. Temperature and concentration profiles for OH, NCO, CN and NH through the flame zone of a CH_4/N_2O flame. The temperature is determined from the spectral fit of the N_2 Stokes Q-branch Raman signal and the concentration data is derived from laser excited fluorescence data.

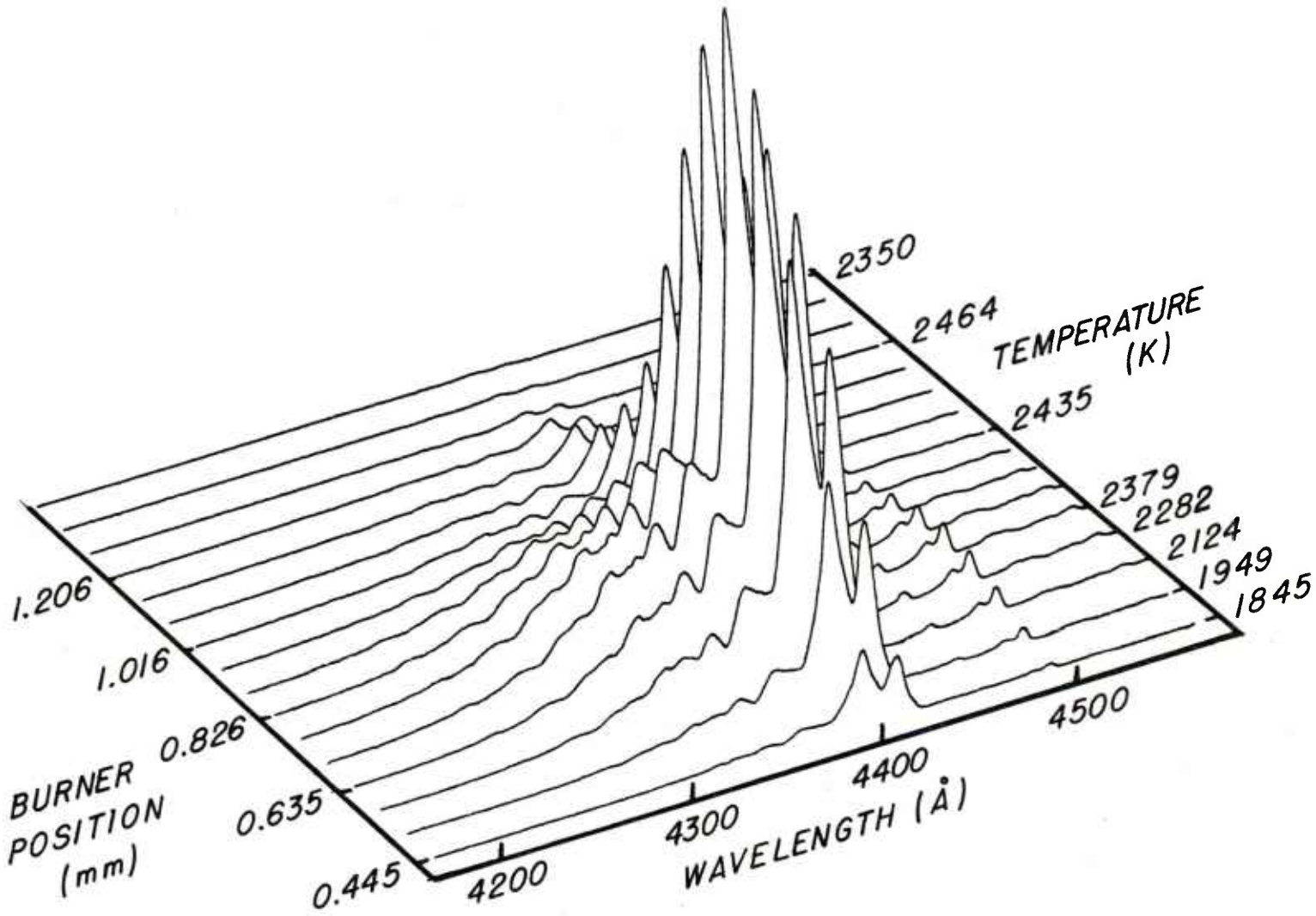

Figure 7. Raw fluorescence spectra of NCO from the reaction zone of a $CH4/N_2O$ flame. The laser excitation wavelength is 4657.95 Å

Nonetheless, normalizing the OH data points in this fashion results in a peak concentration which is 1.7 times larger than the thermochemical equilibrium value. The first two OH data points of Figure 6 have values larger than 3.9×10^{16} molecules/cm^3. However, they were not considered as reliable peak concentration values because here the flame temperature is sharply increasing and any small movement of the flame front has a pronounced effect on the OH concentration through the Boltzmann factor.

The transition which excites NH was not determined. Therefore, an absolute concentration could not be calculated. The thermochemical equilibrium value from the NASA - Lewis code is of no help either since it is almost zero. The estimated value for the NH concentration comes from the work of Anderson, et al.[26] where they measured the NH concentration to be 1.78% of the OH concentration for a stoichiometric CH_4/N_2O_3 flame. Using this ratio and the peak concentration of 3.9×10^{16} molecules/cm^3 for OH, a peak concentration of 1.4×10^{15} molecules/cm^3 is obtained for NH. These radical species concentration profiles are displayed on Figure 6 as a semi-log plot together with the temperature profile plotted linearly. It is difficult to determine the uncertainty of the absolute concentrations of OH and NH when estimated in this fashion. Since the OH concentration is tied to the equilibrium value obtained from the NASA - Lewis code it is probably good to a factor of 2. The NH concentration comes from an OH/NH ratio obtained on another burner operating at lower temperatures; hence,this value is only an order of magnitude estimate. However, the relative concentration profiles have much less uncertainty. If a Boltzmann population distribution is assumed valid, the only major source of uncertainty in determining the relative concentration results from requiring that the quench rate remain constant for the different flame positions sampled.

Assuming effective first order kinetics, the radical species loss rates can be determined from the slope of the profiles when converting burner position to a time scale. The time scale is obtained from the flame gas flow velocity which is 1.62×10^3 mm/sec. These loss rates and standard deviations are listed in Table 4. Loss rates for OH and NCO were also calculated using second order kinetics and the standard deviations were larger for this case, however the precision of the data was not sufficient to assert unambiguously an applicable model. Only relative concentrations are necessary for computing the loss rates. Therefore, the uncertainty in these values should be reasonably described by the standard deviation. Rate constants for these species are computed by dividing the loss rates by the peak concentration values. These values are also listed in Table 4. However, these constants are more uncertain due to the uncertainty in the concentration values.

---

[26] *W. R. Anderson, L. J. Decker and A. J. Kotlar, "Concentration Profiles of NH and OH in a Stoichiometric CH_4/N_2O Flame by Laser Excited Fluorescence and Absorption," Combust. Flame, Vol 48, P. 179, 1982 and Vol. 51, P. 125, 1983.*

TABLE 4. VALUES OF LOSS RATES AND RATE CONSTANTS FOR THE FLAME RADICAL SPECIES ASSUMING FIRST ORDER KINETICS.

Species	Loss Rate (s^{-1})	Concentration (molecules/cm^3)	Rate Constant (cm^3/s)
OH	$2.14 \pm .27 \times 10^2$	3.86×10^{16}	5.54×10^{-15}
NH	$7.12 \pm .58 \times 10^3$	1.35×10^{15}	5.27×10^{-12}
NCO	$1.08 \pm .07 \times 10^4$	3.50×10^{14}	3.08×10^{-11}
CN	$8.73 \pm .43 \times 10^3$	6.26×10^{13}	1.39×10^{-10}

The calculated rate constant for OH using second order kinetics is 7.82×10^{-15} cm^3/sec., somewhat larger than that obtained from first order kinetics but within the estimated uncertainty. Anderson, et al.[24] obtain an OH rate constant of 3.49×10^{-15} cm^3/sec. using second order kinetics for a stoichiometric CH_4/N_2O flame operating at 2200K. This comparison, while not analogous to the present flame conditions, is the closest available. There is a disparity in the equivalence ratios and temperatures. Cattolica[27] has found, however, that the OH rate constant does not vary much for lean to stoichiometric conditions in CH_4/air flames.

With these differences and uncertainty in the absolute concentration of OH, a factor of 2 difference in the comparison is not unexpected.

---

[27] *R. J. Cattolica, "Laser Absorption Measurements of OH in a Methane-Air Flat Flame," Fall Meeting of the Western States Section of the Combustion Institute, Berkeley, California, October 1979, Paper 79-54.*

ACKNOWLEDGEMENT

The authors acknowledge the helpful discussions with D.R. Crosley concerning the spectroscopy of the NH molecule.

REFERENCES

1. D. Crosley, ed., Laser Probes for Combustion Chemistry, ACS Symposium Series 134, 1980.

2. A. C. Eckbreth, "Recent Advances in Laser Diagnostics for Temperature and Species Concentration in Combustion," Proceedings, Eighteenth International Symposium on Combustion, Combustion Institute, Pittsburgh, p. 1471, 1981.

3. D. A. Stephenson, "Non-Intrusive Profiles of Atmospheric Premixed Hydrocarbon-Air Flames," Proceedings, Seventeenth International Symposium on Combustion, Combustion Institute, Pittsburgh, p. 993, 1978.

4. J. A. Vanderhoff, R. A. Beyer and A. J. Kotlar, "Raman Spectroscopy of Premixed CH_4/N_2O and H_2/N_2O Flames," Proceedings, First International Specialists Meeting of the Combustion Institute, Bordeaux, France, Vol.2, Combustion Institute, Pittsburgh, p. 551, 1981.

5. M. Lapp, "Flame Temperatures from Vibrational Raman Scattering," Laser Raman Gas Diagnostics, M. Lapp and C. M. Penney, eds., Plenum Press, New York and London, p. 107, 1974.

6. M. Bridoux, M. Crunelle-Cras, F. Grase and M. Delhaye, "Use of Multichannel Pulsed Raman Spectroscopy as a Diagnostic Technique in Flames," Combust. Flame, Vol. 36, p. 109, 1979.

7. J. H. Bechtel "Laser Probes of Premixed Laminar Methane-Air Flames and Comparison with Theory," Laser Probes for Combustion Chemistry, D. Crosley, ed., ACS Symposium Series 134, p. 85, 1980.

8. R. Cattolica, M. Smooke and A. Dean, "A Hydrogen-Nitrous Oxide Flame Study," Fall Meeting of the Western States Section of the Combustion Institute, Sandia National Laboratories, Livermore, CA, Paper WSS/CI, pp. 82-95, 1982.

9. J. A. Vanderhoff, R. A. Beyer, A. J. Kotlar and W. R. Anderson, "Ar^+ Laser - Excited Fluorescence of C_2 and CN Produced in a Flame," Combust. Flame, Vol. 49, p. 197, 1983.

10. J. A. Vanderhoff, R. A. Beyer, A. J. Kotlar and W. R. Anderson, "Kr^+ and Ar^+ Laser - Excited Fluorescence of CN in a Flame," App. Opt., Vol. 22, p. 1976, 1983.

11. W. R. Anderson, J. A. Vanderhoff, A. J. Kotlar, M. A. Dewilde and R. A. Beyer, "Intracavity Laser Excitation of NCO Fluorescence in an Atmospheric Pressure Flame," J. Chem Phys., Vol. 77, p. 1677, 1982. K. N. Wong, W. R. Anderson, A. J. Kotlar, and J. A. Vanderhoff, to be published.

12. M. Hercher, W. Mueller, S. Klainer, R. F. Adamowicz, R. E. Meyers and S. E. Schwartz, "An Efficient Intracavity Laser Raman Spectrometer," Appl. Spectros., Vol. 32, p. 298, 1978.

13. M. A. Dewilde, Ballistic Research Laboratory Report to be published.

14. R. A. Beyer and M. A. Dewilde, "Simple Burner for Laser Probing of Flames," Rev. Sci. Instr., Vol.53, p. 103, 1982.

15. F. J. Weinberg, Optics of Flames, Butterworth, Inc., Washington, D.C., p. 7, 1963.

16. A. J. Kotlar, Ballistic Research Laboratory Report, to be published.

17. R. A. Svehla and B. J. McBride, "Fortran IV Computer Program for Calculation of Thermodynamic and Transport Properties of Complex Chemical Systems," NASA, TND - 7056, 1973.

18. G. H. Diecke and H. M. Crosswhite, "The Ultraviolet Bands of OH Fundamental Data," J. Quant. Spectrosc. Radiat. Transfer, Vol. 2, p. 97, 1962.

19. R. N. Dixon, "The 0-0 and 1-0 Bands of the $A^3\pi - X^3\Sigma^-$ System of NH," Can. J. Phys., Vol. 37, p. 1171, 1959.

20. (a) G.W. Funke, "Die NH-Banden bei λ 3360," Z. Physik, Vol. 96, p. 787, 1935. (b) G.W. Funke, "Das Absorptionsspektrum des NH," Z Physik, Vol. 101, p. 104, 1936.

21. T. Murai and M. Shimachi, "Rotational Distortions of 3π States Applied to the NH Molecule," Science of Light, Vol. 15, p. 48, 1966.

22. J. J. Cottereau and K. Stepowski, "Laser Induced Fluorescence Spectroscopy Applied to the Hydroxal Radical in Flames," Laser Probes for Combustion Chemistry, D. Crosley, ed., ACS Symposium Series 134, p. 131, 1980.

23. J. H. Bechtel and R. E. Teets, "Hydroxal and Its Concentration Profile in Methane-Air Flames, Appl. Opt., Vol.18, p. 4138, 1979.

24. A. C. Eckbreth, P. A. Bonczyk and J. F. Verdieck, "Laser Raman and Fluorescence Techniques for Practical Combustion Diagnostics", Appl. Spectros. Rev., Vol. 13, p. 52, 1978.

25. W. B. Bridges and A. N. Chester, "Visible and uv Laser Oscillation at 118 Wavelengths in Ionized Neon Argon, Krypton, Xenon, Oxygen and other Gases," Appl. Optics, Vol. 4, p. 573, 1965.

26. W. R. Anderson, L. J. Decker and A. J. Kotlar, "Concentration Profiles of NH and OH in a Stoichiometric CH_4/N_2O Flame by Laser Excited Fluorescence and Absorption," Combust. Flame, Vol 48, p. 179, 1982 and Vol. 51, p. 125, 1983.

27. R. J. Cattolica, "Laser Absorption Measurements of OH in a Methane-Air Flat Flame," Fall Meeting of the Western States Section of the Combustion Institute, Berkeley, California, October 1979, Paper 79-54.

DISTRIBUTION LIST

No. Of Copies	Organization
12	Administrator Defense Technical Info Center ATTN: DTIC-DDA Cameron Station Alexandria, VA 22314
1	Commander US Army Materiel Development and Readiness Command ATTN: DRCDRA-ST 5001 Eisenhower Avenue Alexandria, VA 22333
1	Commander Armament R&D Center USA AMCCOM ATTN: DRSMC-TDC(D) Dover, NJ 07801
1	Commander Armament R&D Center USA AMCCOM ATTN: DRSMC-TSS(D) Dover, NJ 07801
1	Commander US Army Armament, Munitions and Chemical Command ATTN: DRSMC-LEP-L(R) Rock Island, IL 61299
1	Director Benet Weapons Laboratory Armament R&D Center USA AMCCOM Benet Weapons Laboratory ATTN: DRSMC-LCB-TL(D) Watervliet, NY 12189
1	Commander USA Aviation Research and Development Command ATTN: DRDAV-E 4300 Goodfellow Blvd. St. Louis, MO 63120
1	Director USA Air Mobility Research and Development Laboratory Ames Research Center Moffett Field, CA 94035
4	Commander US Army Research Office ATTN: R. Girardelli D. Mann R. Singleton D. Squire Research Triangle Park, NC 27709
1	Commander USA Communications Research and Development Command ATTN: DRSEL-ATDD Fort Monmouth, NJ 07703
1	Commander USA Electronics Research and Development Command Technical Support Activity ATTN: DELSD-L Fort Monmouth, NJ 07703
2	Commander Armament R&D Center USA AMCCOM ATTN: DRSMC-LCA-G(D), D.S. Downs J.A. Lannon Dover, NJ 07801
1	Commander Armament R&D Ctr, USA AMCCOM ATTN: DRSMC-LC(D), L. Harris Dover, NJ 07801
1	Commander Armament R&D Center USA AMCCOM ATTN: DRSMC-SCA-T(D), L. Stiefel Dover, NJ 07801
1	Commander USA Missile Command ATTN: DRSMI-R Redstone Arsenal, AL 35898
1	Commander USA Missile Command ATTN: DRSMI-YDL Redstone Arsenal, AL 35898

DISTRIBUTION LIST

No. Of Copies	Organization
2	Commander USA Missile Command ATTN: DRSMI-RK, D.J. Ifshin Redstone Arsenal, AL 35898
1	Commander USA Tank Automotive Command ATTN: DRSTA-TSL Warren, MI 48090
1	Director USA TRADOC Systems Analysis Activity ATTN: ATAA-SL WSMR, NM 88002
1	Commandant US Army Infantry School ATTN: ATSH-CD-CSO-OR Fort Benning, GA 31905
1	Office of Naval Research Department of the Navy ATTN: R.S. Miller, Code 432 800 N. Quincy Street Arlington, VA 22217
1	Navy Strategic Systems Project Office ATTN: R.D. Kinert, SP 2731 Washington, DC 20360
1	Commander Naval Air Systems Command ATTN: J. Ramnarace, AIR-54111C Washington, DC 20360
3	Commander Naval Ordnance Station ATTN: C. Irish S. Mitchell P.L. Stang, Code 515 Indian Head, MD 20640
1	HQDA(DAMA-ART-M) Washington, DC 20310
1	Commander US Army Development & Employment Agency ATTN: MODE-TED-SAB Fort Lewis, WA 98433

No. Of Copies	Organization
1	Commander Naval Surface Weapons Center ATTN: J.L. East, Jr., G-20 Dahlgren, VA 22448
2	Commander Naval Surface Weapons Center ATTN: R. Bernecker, R-13 G.B. Wilmot, R-16 Silver Spring, MD 20910
4	Commander Naval Weapons Center ATTN: R.L. Derr, Code 389 China Lake, CA 93555
2	Commander Naval Weapons Center ATTN: Code 3891, T. Boggs K.J. Graham China Lake, CA 93555
4	Commander Naval Research Laboratory ATTN: L. Harvey J. McDonald E. Oran J. Shnur Washington, DC 20375
1	Commanding Officer Naval Underwater Systems Center Weapons Dept. ATTN: R.S. Lazar/Code 36301 Newport, RI 02840
1	Superintendent Naval Postgraduate School Dept. of Aeronautics ATTN: D.W. Netzer Monterey, CA 93940
5	AFRPL (DRSC) ATTN: R. Geisler D. George D. Weaver J. Levine W. Roe Edwards AFB, CA 93523

DISTRIBUTION LIST

No. Of Copies	Organization
1	AFATL/DLDL ATTN: O.K. Heiney Eglin AFB, FL 32542
1	AFOSR ATTN: L.H. Caveny Bolling Air Force Base Washington, DC 20332
1	AFWL/SUL Kirtland AFB, NM 87117
1	NASA Langley Research Center ATTN: G.B. Northam/MS 168 Hampton, VA 23365
4	National Bureau of Standards ATTN: J. Hastie M. Jacox T. Kashiwagi H. Semerjian US Department of Commerce Washington, DC 20234
1	Aerojet Solid Propulsion Co. ATTN: P. Micheli Sacramento, CA 95813
1	Applied Combustion Technology, Inc. ATTN: A.M. Varney P.O. Box 17885 Orlando, FL 32860
2	Atlantic Research Corp. ATTN: M.K. King 5390 Cherokee Avenue Alexandria, VA 22314
1	Atlantic Research Corp. ATTN: R.H.W. Waesche 7511 Wellington Road Gainesville, VA 22065
1	Battelle Memorial Institute Tactical Technology Center ATTN: J. Huggins 505 King Avenue Columbus, OH 43201
2	Exxon Research & Eng. Co. ATTN: A. Dean M. Chou P.O. Box 45 Linden, NJ 07036
1	Ford Aerospace and Communications Corp. DIVAD Division Div. Hq., Irvine ATTN: D. Williams Main Street & Ford Road Newport Beach, CA 92663
1	General Electric Armament & Electrical Systems ATTN: M.J. Bulman Lakeside Avenue Burlington, VT 05401
1	General Electric Company ATTN: M. Lapp Schenectady, NY 12301
1	AVCO Everett Rsch. Lab. Div. ATTN: D. Stickler 2385 Revere Beach Parkway Everett, MA 02149
1	General Motors Rsch Labs Physics Department ATTN: J.H. Bechtel Warren, MI 48090
3	Hercules, Inc. Alleghany Ballistics Lab. ATTN: R.R. Miller P.O. Box 210 Cumberland, MD 21501

DISTRIBUTION LIST

No. Of Copies	Organization
1	University of Southern California Dept. of Chemistry ATTN: S. Benson Los Angeles, CA 90007
1	Case Western Reserve Univ. Div. of Aerospace Sciences ATTN: J. Tien Cleveland, OH 44135
1	Cornell University Department of Chemistry ATTN: E. Grant Baker Laboratory Ithaca, NY 14853
1	Univ. of Dayton Rsch Inst. ATTN: D. Campbell AFRPL/PAP Stop 24 Edwards AFB, CA 93523
1	University of Florida Dept. of Chemistry ATTN: J. Winefordner Gainesville, FL 32601
3	Georgia Institute of Technology School of Aerospace Engineering ATTN: E. Price Atlanta, GA 30332
2	Georgia Institute of Technology School of Aerospace Engineering ATTN: W.C. Strahle B.T. Zinn Atlanta, GA 30332
1	University of Illinois Dept. of Mech. Eng. ATTN: H. Krier 144MEB, 1206 W. Green St. Urbana, IL 61801
1	Johns Hopkins University/APL Chemical Propulsion Information Agency ATTN: T.W. Christian Johns Hopkins Road Laurel, MD 20707
1	University of Minnesota Dept. of Mechanical Engineering ATTN: E. Fletcher Minneapolis, MN 55455
4	Pennsylvania State University Applied Research Laboratory ATTN: G.M. Faeth K.K. Kuo H. Palmer M. Micci University Park, PA 16802
1	Polytechnic Institute of NY ATTN: S. Lederman Route 110 Farmingdale, NY 11735
2	Princeton University Forrestal Campus Library ATTN: K. Brezinsky I. Glassman P.O. Box 710 Princeton, NJ 08540
1	Princeton University MAE Dept. ATTN: F.A. Williams Princeton, NJ 08544

DISTRIBUTION LIST

No. Of Copies	Organization
2	Purdue University School of Aeronautics and Astronautics ATTN: R. Glick J.R. Osborn Grissom Hall West Lafayette, IN 47907
3	Purdue University School of Mechanical Engineering ATTN: N.M. Laurendeau S.N.B. Murthy D. Sweeney TSPC Chaffee Hall West Lafayette, IN 47906
1	Rensselaer Polytechnic Inst. Dept. of Chemical Engineering ATTN: A. Fontijn Troy, NY 12181
2	Southwest Research Institute ATTN: R.E. White A.B. Wenzel 8500 Culebra Road San Antonio, TX 78228
1	Stanford University Dept. of Mechanical Engineering ATTN: R. Hanson Stanford, CA 94305
2	University of Texas Dept. of Chemistry ATTN: W. Gardiner H. Schaefer Austin, TX 78712
1	University of Utah Dept. of Chemical Engineering ATTN: G. Flandro Salt Lake City, UT 84112
1	Virginia Polytechnic Institute and State University ATTN: J.A. Schetz Blacksburg, VA 24061
	Aberdeen Proving Ground
	Dir, USAMSAA ATTN: DRXSY-D DRXSY-MP, H. Cohen Cdr, USATECOM ATTN: DRSTE-TO-F Cdr, CRDC, AMCCOM ATTN: DRSMC-CLB-PA DRSMC-CLN DRSMC-CLJ-L

USER EVALUATION SHEET/CHANGE OF ADDRESS

This Laboratory undertakes a continuing effort to improve the quality of the reports it publishes. Your comments/answers to the items/questions below will aid us in our efforts.

1. BRL Report Number _____ Date of Report _____

2. Date Report Received _____

3. Does this report satisfy a need? (Comment on purpose, related project, or other area of interest for which the report will be used.) _____

_____

_____

4. How specifically, is the report being used? (Information source, design data, procedure, source of ideas, etc.) _____

_____

_____

5. Has the information in this report led to any quantitative savings as far as man-hours or dollars saved, operating costs avoided or efficiencies achieved, etc? If so, please elaborate. _____

_____

_____

6. General Comments. What do you think should be changed to improve future reports? (Indicate changes to organization, technical content, format, etc.)

_____

_____

_____

CURRENT ADDRESS

_____
Name

_____
Organization

_____
Address

_____
City, State, Zip

7. If indicating a Change of Address or Address Correction, please provide the New or Correct Address in Block 6 above and the Old or Incorrect address below.

OLD ADDRESS

_____
Name

_____
Organization

_____
Address

_____
City, State, Zip

(Remove this sheet along the perforation, fold as indicated, staple or tape closed, and mail.)